Journal of Geophysical Research: Biogeosciences

RESEARCH ARTICLE
10.1029/2018JG004392

Key Points:
- In the Eastern Tropical North Pacific large, fast-sinking, organic particles were refractory and not formed directly from phytoplankton cells
- Particle aggregation occurred over time through the initial formation of smaller, suspended, and slow-sinking particles
- This alternative particle formation has not been previously described and likely persists where small phytoplankton species dominate

Supporting Information:
- Supporting Information S1

Correspondence to:
E. L. Cavan,
emma.cavan@utas.edu.au

Citation:
Cavan, E. L., Giering, S. L. C., Wolff, G. A., Trimmer, M., & Sanders, R. (2018). Alternative particle formation pathways in the Eastern Tropical North Pacific's biological carbon pump. *Journal of Geophysical Research: Biogeosciences*, *123*, 2198–2211. https://doi.org/10.1029/2018JG004392

Received 14 JAN 2018
Accepted 8 JUN 2018
Accepted article online 26 JUN 2018
Published online 24 JUL 2018

Alternative Particle Formation Pathways in the Eastern Tropical North Pacific's Biological Carbon Pump

E. L. Cavan[1,2,3], S. L. C. Giering[1], G. A. Wolff[4], M. Trimmer[5], and R. Sanders[1]

[1]National Oceanography Centre, European Way, Southampton, UK, [2]National Oceanography Centre, University of Southampton, Southampton, UK, [3]Now at Institute for Marine and Antarctic Studies, University of Tasmania, Tasmania, Australia, [4]School of Environmental Sciences, University of Liverpool, Liverpool, UK, [5]School of Biological and Chemical Sciences, Queen Mary University London, London, UK

Abstract A fraction of organic carbon produced in the oceans by phytoplankton sinks storing 5–15 gigatonnes of carbon annually in the ocean interior. The accepted paradigm is that rapid aggregation of phytoplankton cells occurs, forming large, fresh particles which sink quickly; this concept is incorporated into ecosystem models used to predict the future climate. Here we demonstrate a slower, less efficient export pathway in the Eastern Tropical North Pacific. Lipid biomarkers suggest that the large, fast-sinking particles found beneath the mixed layer are compositionally distinct from those found in the mixed layer and thus not directly and efficiently formed from phytoplankton cells. We postulate that they are formed from the in situ aggregation of smaller, slow-sinking particles over time in the mixed layer itself. This export pathway is likely widespread where smaller phytoplankton species dominate. Its lack of representation in biogeochemical models suggests that they may be currently overestimating the ability of the oceans to store carbon if large, fast-sinking, labile particles dominate simulated particle export.

Plain Language Summary The oceans are one of the largest sinks of atmospheric carbon dioxide on our planet. One method by which this occurs is through the production of organic material (phytoplankton—plant-like cells) in the surface ocean, which capture atmospheric carbon dioxide during photosynthesis. Eventually, the phytoplankton die and sink out of the surface ocean, transporting huge amounts of carbon to the deep ocean where it is stored for centuries or even millennia. Our current understanding is that generally, most organic material sinks quickly as large, fast-sinking (hundreds of meters per day) particles (clumps of dead phytoplankton cells). However, in our study in the Equatorial Pacific Ocean, we were able to show that a different and much slower process occurs where phytoplankton first aggregate to smaller, slower sinking detrital particles and eventually form very degraded larger particles that sink to the deep. This has consequences for estimating ocean carbon storage as smaller particles are respired much quicker than larger particles. Thus, where they are an important part of this carbon sink, such as in the Equatorial Pacific, the proportion phytoplankton-captured atmospheric carbon dioxide being stored in the deep ocean is likely reduced.

1. Introduction

Organic matter transferred to depth via sinking particles as part of the biological carbon pump affects the oceans in two ways: (1) It is the main food source of heterotrophs in the deep ocean (Eppley & Peterson, 1979; Graf, 1989), and (2) it can sequester carbon for hundreds or thousands of years, away from exchange with the atmosphere (Kwon et al., 2009; Parekh et al., 2006; Volk & Hoffert, 1985). Our current understanding is that phytoplankton (which convert inorganic carbon to organic carbon), bacterioplankton, and zooplankton interact in the mixed layer, leading to the formation of large detrital particles that sink quickly through the mixed layer and into the deep ocean (Billett et al., 1983; Buesseler et al., 2001; Volk & Hoffert, 1985). This concept stems predominantly from work in higher latitudes such as the seasonally productive North Atlantic, where clumps of "phytodetritus" (large, green, fresh organic particles) have been observed at the seafloor at depths greater than 2,000 m (Billett et al., 1983). This results from a high proportion (40%) of phytoplankton production being exported from euphotic zone and quick and efficient transfer to depth (Buesseler et al., 1992). Efficient transfer also occurs in the Southern Ocean by diatoms (large phytoplankton) as relatively intact diatoms have been found in deep sediment traps and marine sediments (Salter et al., 2012; Wakeham et al., 1979; Zielinski & Gersonde, 1997).

Recently, we showed that where in situ oxygen concentrations are low, such as in the Eastern Tropical North Pacific (ETNP), the transfer efficiency (proportion of exported particles reaching the deep ocean) of large, fast-sinking particles is high, relative to other regions (Cavan, Trimmer, et al., 2017). We proposed that reduced zooplankton-particle interactions in the low oxygen waters were largely responsible. Still, there were uncertainties as to how these larger, fast-sinking particles formed. We found that the flux of smaller, slow-sinking particles was at times as large as the fast-sinking flux but was remineralized and thus attenuated with depth, much more rapidly. This was due to the faster particulate organic carbon (POC) turnover by microbes on the smaller particles due to their large surface area-to-volume ratio (Cavan, Trimmer, et al., 2017).

Slow-sinking particles, both in and immediately below the mixed layer, are ubiquitous in the global oceans; however, their importance in export flux varies regionally (Baker et al., 2017; Cavan, Henson, et al., 2017; Durkin et al., 2015; Riley et al., 2012). In lower latitude environments such as south of the Canary Current in the Atlantic Ocean slow-sinking particles can contribute to a larger part of the particle flux than fast-sinking particles for at least half the year (Alonso-Gonzalez et al., 2010). Current understanding from middle- to high-latitude studies suggests that slow-sinking particles found beneath the mixed layer originate from the in situ fragmentation and disaggregation of larger, fast-sinking particles (Baker et al., 2017; Giering et al., 2014; Mayor et al., 2014). Future projections of export from the upper ocean highlight that the greatest discrepancies in export production between models derive from uncertainty and variability in particle formation (Laufkötter et al., 2016), meaning that detailed information of particle formation processes in different biomes is of critical importance. Hence, we endeavored to track the particle composition through suspended, slow-, and fast-sinking particles to shed light on particle formation pathways in the equatorial Pacific.

Conventional tracers of flux, such as sediment and gel traps, cannot yield such information as particles are collected on long timescales (days to months) and settle on top of each other; hence, once collected, they are no longer in their original form. This means that indirect traces of formation processes such as source-specific lipid biomarkers (Wakeham & Canuel, 1988) are useful to allow comparison of particle composition across all sinking fractions regardless of size, below the limit at which light microscopy can elucidate their formation processes ($\sim<100$ μm). Lipids have a wide range of biochemical functions, for example, in energy storage and in acting as structural components of cell walls. They are structurally diverse and have some source specificity, hence can be useful as biomarkers (Volkman et al., 1998). They also have differing environmental stability, with certain compounds being rather labile (e.g., polyunsaturated fatty acids; Zimmerman & Canuel, 2001), while others are more refractory (e.g., sterols; Kiriakoulakis et al., 2004; Sheridan et al., 2002; Zimmerman & Canuel, 2001). So in the ocean the lipid composition of particulate organic matter depends on the original source phytoplankton and the processes undergone through the water column such as senescence, ingestion by heterotrophs, and bacterial degradation (Sheridan et al., 2002).

According to our current understanding based on middle- to high-latitude studies and implemented in models, we expect fast-sinking particles (phytodetrital aggregates and fecal pellets) to be labile and similar in lipid composition to particles in the mixed-layer (mostly viable phytoplankton cells), whereas slow-sinking particles, as the degradation products of the fast-sinking particles, should be more refractory with a different lipid profile. Nevertheless, organic particle composition studies at lower latitudes, such as the Mediterranean and equatorial Pacific, have shown suspended particles to be very labile, whereas larger, sinking particles are more degraded due to intense alteration (Abramson et al., 2010; Alonso-Gonzalez et al., 2010; Puigcorbé et al., 2015; Wakeham & Canuel, 1988). It should be noted that in some studies particle fractions were collected using different methods (pumps versus sediment traps), at different depths and over different time frames (hours to days), making it difficult to compare the particle fractions.

In this study, we were able to collect and measure the lipid composition of suspended, slow- and fast-sinking particles using the same sampling device (Marine Snow Catchers, MSCs), so all exported particle fractions were from the same depth and captured over the same time period. MSCs act like large (300 L volume, 2 m height) Niskin bottles used as a large settling columns on deck to collect particles of different sinking rates. See section 2 for more information on the MSC. Here we used MSCs in the upper mesopelagic zone (40–350 m) to collect suspended, fast- and slow-sinking particles in the low-latitude ETNP. We used particulate lipids as biomarkers to track the changes in composition between fast-, slow-sinking and suspended particles to elucidate particle formation pathways. We then collected water from the mixed layer ($<$40 m) using Niskin bottles (essentially smaller MSCs not left to settle) to compare particle composition between exported

and mixed layer particles. We also measured the size of fast- and slow-sinking particles to test the assumption that slow-sinking particles are smaller than fast-sinking particles.

2. Methods

2.1. Cruise Location

Particles were collected from the ETNP on board the RRS *James Cook* from 28 December 2013 to 10 February 2014. There were six stations along a transect (Figure 1a). At each station a conductivity-temperature-depth sensor (Seabird 11 plus) attached to a Rosette was deployed with a fluorometer (Chelsea Aqua Tracker III) to measure chlorophyll *a* to determine particle sampling depths. Chlorophyll *a* was also measured by collecting 500 mL of seawater from the Niskin bottles throughout the upper 100 m and filtering through a glass fiber (GF/F) filter of 0.7-m pore size. Individual filters were then submerged in 90% acetone to extract the chlorophyll *a* and placed in the fridge the overnight. The filter was removed and the acetone placed in a fluorometer (Turner trilogy) to determine chlorophyll *a* concentration in $\mu g\ L^{-1}$. In addition, mean sea surface chlorophyll *a* data for the month of January 2014 were downloaded from aqua MODIS satellite to derive surface concentrations at each station and the surrounding waters in the ETNP (Figure 1a).

2.2. Particle Collection, Size, and Sinking Rates

Giant (300-L total volume compared to 95 L in the standard devices) MSCs were used to collect sinking and suspended particles from the upper mesopelagic zone (<400 m). The MSC is a polyvinyl chloride water sampler similar to a Niskin bottle but with a removable base section which holds ~ 35 L of the total water volume (Figure S1 in the supporting information). During deployment, the two ends are manually closed at a discrete depth and then bought back on deck within 30 min, depending on the depth sampled. The water and particles at this point in the MSC represent a homogenous and well-mixed water column. The MSC is then used as a settling column to separate particles of different sinking rates. On deck the water in the MSC is left to settle for 2 hr such that post settling the particles collected on the base of the MSC are defined as fast-sinking ($>20\ m\ d^{-1}$) particles, those collected just above the base are slow-sinking ($<20\ m\ d^{-1}$), and those within the main body of the MSC are suspended particles ($0\ m\ d^{-1}$; see Riley et al., 2012 for more information on the MSC). The sinking rate definitions are calculated from the height of the MSC and the time left to settle as described in Riley et al. (2012). On the Giant MSCs used in this study, there is one tap at the bottom of the base and multiple ones running the length of the top section (Figure S1). After 2 hr suspended particles are sampled from the top section (middle tap), slow-sinking from the base tap and fast-sinking from the base tray sat at the very bottom of the MSC (see Figure S1 for schematic of MSC and more detailed sampling protocol). It is noteworthy though that slow-sinking particles—by definition—also include suspended particles. Particles collected using MSCs can then be used in onboard laboratory incubations (Belcher, Iversen, Giering, et al., 2016; Belcher, Iversen, Manno, et al., 2016; Cavan, Trimmer, et al., 2017), for particle flux quantification (Baker et al., 2017) and settling rates (Becquevort & Smith, 2001), and particle identification (Cavan et al., 2015) or for particle composition analysis (Giering et al., 2017; Riley et al., 2012).

Deployment depths ranged from 10 m below the subsurface chlorophyll maximum (as determined from prior conductivity-temperature-depth casts equipped with a fluorescence sensor) to 350-m water depth. At each of the six stations four depths were sampled using the MSCs. The shallowest was always 10 m below the chlorophyll maximum and the deepest depended on the depth of the water column (110–3,000 m) but never exceeded 350 m. After collection, the particulate matter was allowed to settle for 2 hr before being sampled. A full-range, mixed sample of particulate matter of all particle fractions (i.e., all sinking/suspended fractions) from the upper mixed layer (10–30 m, mixed layer depth = 40 m) was collected using Niskin bottles (20 L) attached to a Rosette frame an filtered immediately on deck.

Fast-sinking rates and particle size (equivalent spherical diameter, ESD) were estimated using a FlowCam (Bach et al., 2012) to test for a relationship between particle size and sinking rate and characterize the size of fast- and slow-sinking particles. Fast-sinking particles were placed in a funnel suspended above a flow cell, the two being connected by tubing (10-mm internal diameter). The funnel, tube, and flow cell were filled with filtered seawater (0.2-μm polycarbonate filter) collected using Niskin bottles and the particles introduced using a truncated Pasteur pipette (opening ~5 mm). The particles were placed in the funnel and allowed to settle through the tube and flow cell at their natural sinking rate. We were able to do these

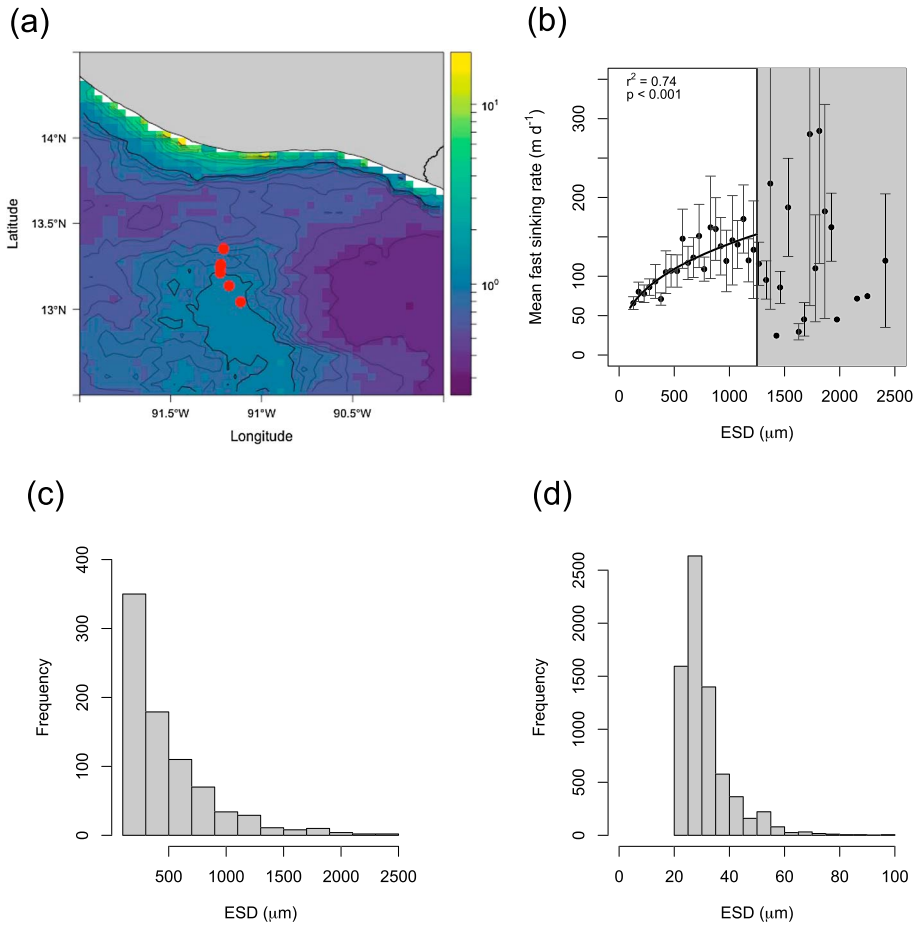

Figure 1. Sampling locations and particle size and sinking rate in the Eastern Tropical North Pacific. (a) Mean monthly surface chlorophyll *a* concentrations for January 2014, taken from National Oceanic and Atmospheric Administration Moderate Resolution Imaging Spectroradiometer satellite data. The gray continent is the Pacific coast of Guatemala, and the red points are sampling locations. (b) Sinking rate of fast-sinking particles against equivalent spherical diameter (ESD). The mean sinking rate (binned for 50-μm ESD size classes) and standard error of the mean are presented ($n = 810$). There is a significant ($p < 0.001$) relationship between ESD and sinking rate for particles between 100 and 1,250 μm; above this, the relationship breaks down (gray rectangle). (c and d) Histograms of ESD for fast-sinking (200-μm size bins, $n = 810$) and slow-sinking particles (5-μm size bins, $n = 7,170$), respectively.

measurements on the ship as the water in the ETNP was flat calm (sea state = 0 to 1) during the entire 7-week voyage. On-board ship temperatures were higher than in situ. We corrected for the effect of temperature by assuming that an increase in sea-water temperature of 9 °C results in a 40% increase in sinking rate (Bach et al., 2012). Sinking rates were calculated from the number of images of individual particles; the time interval images were taken as well as the vertical distance of the flow cell. Particles that were collected as part of the fast-sinking fraction but sank at rates <20 m d^{-1} (5% by volume) were not included in the sinking rate statistics as these are by definition slow-sinking particles. ESD was calculated from the images based on the mean of 36 feret measurements every 5°. Water containing slow-sinking particles was also injected into the FlowCAM to measure slow-sinking particle ESD. One particle sank at 33 m d^{-1} and is by our definition a fast-sinking particle; thus, we excluded it from our fast-sinking particle analyses because of its anomalously small size ($<$mean $-$ 2 $\times$ standard deviations) and it being the only fast sinking particle smaller than 100 μm (Figure 1).

2.3. Particle Composition

The morphological composition of the fast-sinking particles (as either phytodetrital aggregates or fecal pellets) was quantitatively determined at 100× magnification using an Olympus microscope. A more in-depth,

qualitative, compositional analysis was carried out using high magnification (1,000×) FlowCAM images. Slow-sinking particles were too small (~30 μm ESD) and heterogeneous to allow identification of their type or origin; hence, lipid composition was used to determine the nature of all particles for comparison.

For particulate lipid composition analysis, one fourth (600 mL) of the MSC base tray (for fast-sinking particles) and 2 L of each sample of mixed-layer, suspended and slow-sinking particles were filtered through precombusted (400 °C, overnight) GF/F filters, which were frozen at −80 °C onboard the ship and then freeze-dried on return to the laboratory. Analyses of lipids were carried out according to Kiriakoulakis et al. (2004). Briefly, filters were spiked with an internal quantification standard (5 μL of 5αH-cholestane in cyclohexane 101.42 ng L^{-1}) and a solvent mixture of dichloromethane : methanol (9:1, 3 mL) added to the filters in a glass centrifuge tube (60 mL). The tubes were sonicated (30 min) and centrifuged (5 min, at 2,500 rpm, 15 °C) and the solvent evaporated using a rotary evaporator. The total lipid extract (TLE) was transferred to a Reacti-vial, and the sample was transmethylated using acetylchloride : methanol (1:40, 1 mL) and kept at 45 °C in the dark overnight. The TLE was then neutralized by passing through a potassium carbonate column (Pasteur pipette). Finally, the TLE was derivatized with 25 μL of BSTFA (*bis*-trimethylsilyl-trifluoroacetamide) and the samples stored in a freezer at −20 °C until analysis.

The samples were analyzed first using a gas chromatograph (GC; Agilent 5890 FID; 30-m DB5MS, J&W Ltd, He carrier gas 1.2 mL min^{-1}) to check their quality and then by GC-mass spectrometry (GCMS Thermoquest Finnigan TSQ7000; Trace 2000 GC, on column injection, 60-m DB5MS, J&W Ltd, He carrier gas 1.6 mL min^{-1}, oven programmed 60 °C to 170 °C at 6 °C min^{-1} after 1 min, then to 315 °C at 2.5 °C min^{-1} and held for 10 min, transfer line 320 °C, source 230 °C, EI 70 eV, trap current 300 μA, Full Data Acquisition mode). Xcalibur software was used to receive and process the data from the GCMS. Compounds were quantified by comparison of the peak areas of the internal standard (5αH-cholestane) with that of the compound of interest and corrected by their relative response factors.

Fatty acids (saturated, branched, and unsaturated, C14–C26), alcohols, and sterol compounds were identified and quantified. Lipid mass (ng) was converted to concentration by dividing by the volume of water filtered. Concentrations were also normalized to POC (determined from CHN elemental analysis) to determine the percentage contribution of lipids to POC. The lowest concentration of total lipids measured was 0.9 ng L^{-1}, hence the lowest threshold of reliable lipid quantification. The mean proportion of the most abundant lipids for each fraction (Figure 3 and Table S3 in the supporting information) was computed. Data were square-root transformed, and a Bray-Curtis dissimilarity matrix was used to produce numerical multidimensional scaling (NMDS) plots. Multivariate statistical analyses were computed to identify the degree of dissimilarity of lipid compositions between particle fractions (Adonis, nonparametric multivariate analysis of variance; Anderson, 2001). The Adonis tests for differences (dissimilarities) in centroids of lipid compositions between each particle fraction (see NMDS plots). This test assumes that the observations have similar distributions so we used a PERMANOVA (beta dispersion test) to test this assumption. Both tests were run in R (R Development Core Team, 2017) using the "Vegan" package. All errors presented in this study are one standard error of the mean.

3. Results

3.1. Particle Size and Sinking Rates

Fast-sinking particles ranged in ESD from 100 to 2,500 μm, with a mean ESD of 488 ± 14 μm (n = 810, Figures 1c and 1d). They were generally smaller than typical "marine snow" defined as >0.5-mm ESD (Alldredge & Gotschalk, 1988) observed at middle to high latitudes, with 65% of fast-sinking particles at the ETNP being <500 μm. This smaller particle size reflects the smaller phytoplankton species found here (Malone, 1971) compared to temperate and polar waters where larger phytoplankton dominate production. Mixed layer chlorophyll *a* concentrations were moderate with a maximum of 3.3 μg L^{-1} at station 6 (furthest offshore, Figure S2), which confirms that the ETNP is not an oligotrophic system.

For fast-sinking particles with an ESD < 1,250 μm, we found a significant relationship between their size (ESD) and sinking rate (R^2 = 0.74; p < 0.001; n = 665; Figure 1b). For fast-sinking particles >1,250 μm in ESD, this relationship broke down (p = 0.89), perhaps because of the small sample size of very large particles (n = 56), or because the flow cell in the FlowCAM, used for making the sinking rate measurements, was

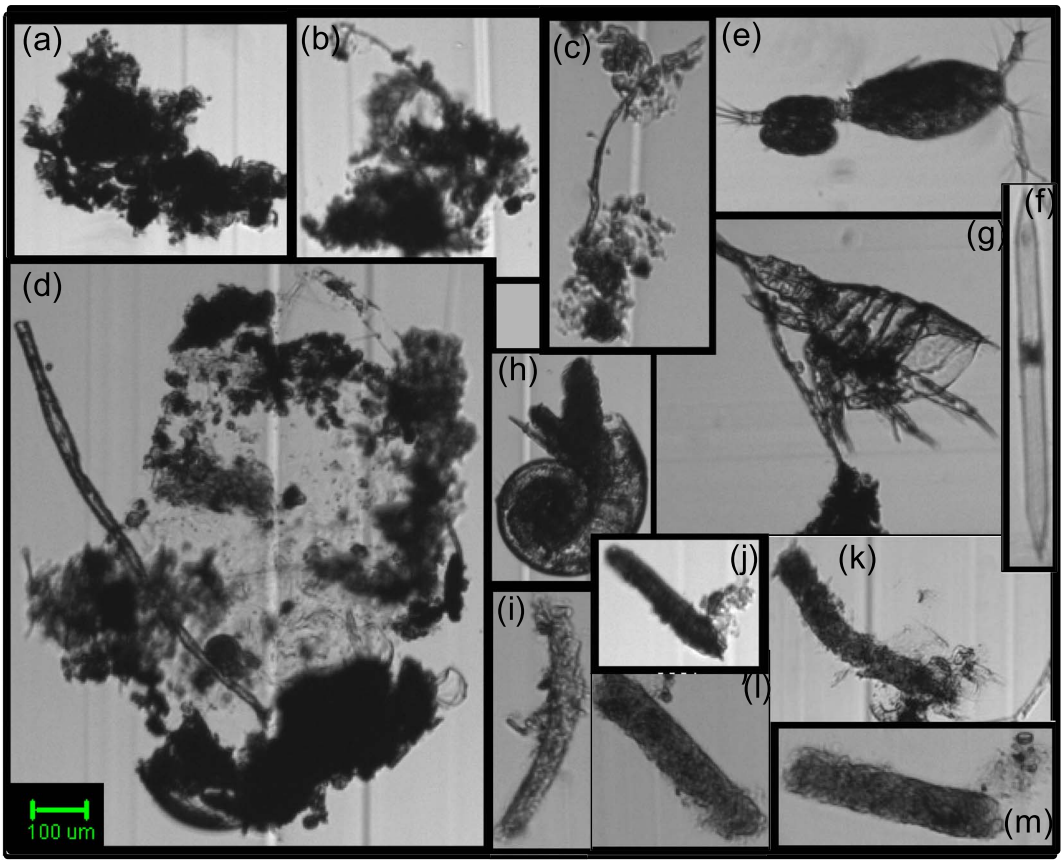

Figure 2. Images of particles from each type identified taken using the FlowCAM. (a–d) Phytodetrital aggregates; (d) is classed as a particle visibly containing gelatinous material; (e) Copepod carcass, (f) a diatom, (g) a zooplankton-shed carapace, and (h) a pteropod; (i–m) zooplankton fecal pellets. All images are scaled corrected to the 100-μm scale bar in the bottom right-hand corner.

only 800 μm deep (but ~5 mm wide), restricting the free sinking of very large particles. The sinking rate range of all fast-sinking particles was 20–715 m d^{-1} with a mean of 129 (±5) m d^{-1} (n = 810). It was not possible to calculate individual sinking rates for slow-sinking particles (<20 m d^{-1}) because of their small size. They were significantly smaller than fast-sinking particles ($p < 0.001$, t test, mean ESD = 31 ± 0.13, n = 7,170) and ranged between 20 and 200 μm (Figure 1d), so that the size distributions for the two sinking fractions were almost distinct, with some overlap between 100 and 200 μm (Figures 1c and 1d).

Fast-sinking particles were dominated by phytoplankton detrital aggregates (65%, Figures 2a–2d), followed by fecal pellets (14%, Table S1), which together, comprised 79% of the fast-sinking fraction. Fecal pellets were likely produced by copepods as we found dead copepods and their exoskeletons in our particulate samples (Figures 2e and 2g). On average (mean ± standard error of the mean) fecal pellets sank slower (80 ± 15 m d^{-1}, n = 114) than aggregates (104 ± 9 m d^{-1}, n = 530, Table S1). The fastest sinking particles were pteropods (296 ± 123 m d^{-1}, n = 4), but this rate was based on just four samples. We estimated that gelatinous aggregates (e.g., Figure 2d) made up 7% of fast-sinking particles but consider this an underestimate due to the transparent nature of most gelatinous material.

3.2. Particle Composition

Even though phytodetrital aggregates dominated particle abundance, there were no lipid biomarkers typical of larger phytoplankton species in any of the samples (eicosapentaenoic acid for diatoms and docosahexaenoic acid for dinoflagellates; Kates & Volcani, 1966; Mansour et al., 1999), implying that other phytoplankton dominated the community composition in the ETNP. Cyanobacteria are typically abundant (up to 160 × 10^6 cells L^{-1}) in the ETNP (Goericke et al., 2000) and characterized by high amounts of $C_{16:0}$, $C_{16:1}$,

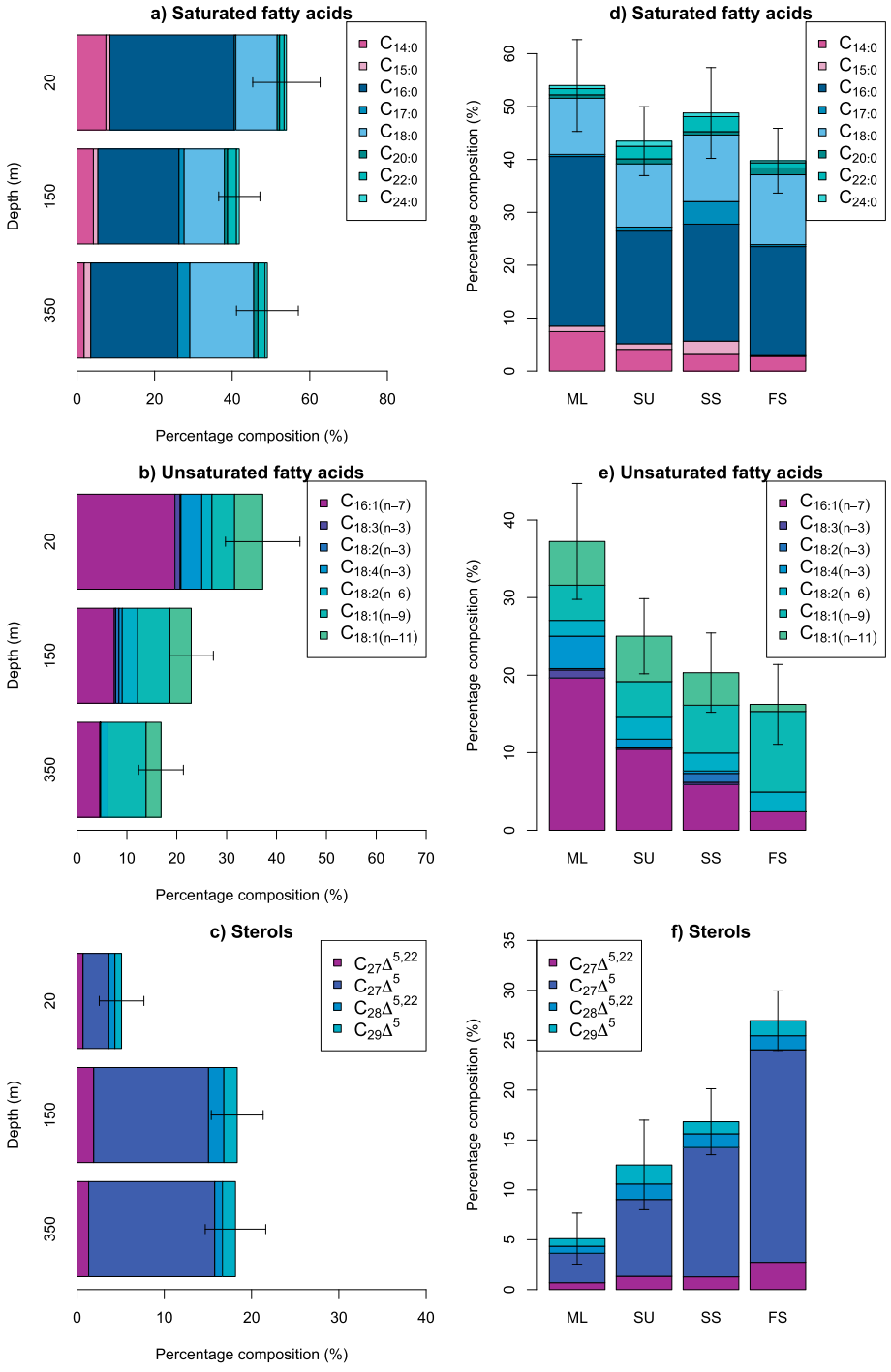

Figure 3. Mean particulate lipid compositions for saturated, unsaturated and sterols. (a–c) Composition across particle fractions; ML = mixed layer, SU = suspended, SS = slow sinking, FS = fast sinking. SU, SS, and FS are exported particles. (d–f) Composition with depth. The bar at 20 m (a–c) is the same data and output as the ML bar in (d)–(f) and represents lipid collected using Niskin bottles. The 150-m bar represents mean particle lipids from below the mixed layer (>40 m) to 150 m and the 350-m bar from 151 to 350 m. The error bars are standard error of the mean. See Table S2 for lipid nomenclature and Table S3 for data. The changes in lipid compositions with depth are consistent with previous findings. The differences between the particle fractions show that the mixed layer particles were dominated by fresh, labile unsaturated-fatty acids but fast-sinking particles by refractory, heterotrophic sterols. The greatest different in lipid composition was between mixed layer and fast-sinking particles.

Table 1
Results of Multivariate Statistical Analyses (Adonis and Beta Dispersion) Between Lipid Compositions of Each Particle Fraction as Presented in Figure 4

Fraction 1	Fraction 2	n	Beta dispersion		Adonis	
			F statistic	*p*	R^2	*p*
ML	SU	23	3.11	0.11	0.13	0.01
ML	SS	28	16.25	0.00	0.17	0.00
ML	FS	27	6.80	0.03	0.32	0.00
SU	SS	29	10.41	0.00	0.08	0.04
SU	FS	28	2.29	0.15	0.22	0.00
SS	FS	33	4.42	0.06	0.07	0.02

Note. ML = mixed layer, SU = suspended, SS = slow-sinking, FS = fast-sinking particles. *n* is the number of samples per test with a total of 56 samples analyzed, where $p > 0.05$ in the beta dispersion test is when the assumptions were met for the Adonis test to be certain differences in dispersion (variance) are not causing the Adonis result. Nevertheless, we consider highly significant Adonis results (where $p = 0.00$, e.g., between ML and FS) to present true differences in lipid compositions even if the dispersions were also different.

and $C_{18:1}$ fatty acids (Wakeham, 1995), typically in the ratio 1:1.3:4, respectively (Sallal et al., 1990). In our samples these fatty acids follow a similar distribution; 1:1.5:6 with $C_{16:0}$ contributing 20–32% to total lipid composition (0.003–3.8 μg L^{-1}), $C_{16:1}$ 4–20% (0.005–4.4 μg L^{-1}), and $C_{18:1}$ 1–10% (0.006–2.2 μg L^{-1}), emphasizing the likely dominance of cyanobacteria in the ETNP during our study. The common crustaceous zooplankton lipid biomarkers ($C_{20:1}$ and $C_{22:1}$ alcohols or fatty acids; Dalsgaard et al., 2003) were below the detection limits in our samples, even though we observed the presence of copepods in some of our samples.

Lipids only contributed 1.4% (±0.01%) of POC on average (range 0.04–10%), suggesting that other types of carbon-rich compounds (e.g., carbohydrates) made up the largest part of the fast-sinking particles. There was little change in saturated fatty acid contributions to total lipids (%) with depth (Figure 3a); however, the more labile unsaturated fatty acids typically synthesized during primary production (Zimmerman & Canuel, 2001) decreased in relative abundance by at least 50% from the mixed layer to 350 m (Figure 3b). In contrast, sterols dominated by cholesterol were very low in relative abundance (3% of total lipids) in the mixed layer (10–30 m) and much more abundant in exported particles (8–21%, 40–350 m, Figure 3c). However, we show here that across the four different particle fractions (full-range of mixed layer and exported suspended, slow- and fast-sinking particles) there was little change in the magnitude of saturated fatty acids to total lipids (Figure 3d), but unsaturated fatty acids decreased and sterols increased in relative abundance sequentially across the four particle fractions from mixed-layer > suspended > slow-sinking > fast-sinking particles (Figures 3e and 3f).

We applied a multivariate analysis of variance to identify the strongest dissimilarities between the particle fractions (Adonis test, Table 1). In this test, the value of R^2 represents the strength of dissimilarities between two groups, with a high R^2 representing distinctly different groups and a low R^2 specifying very similar groups. The Adonis test assumes that dispersions of samples are similar between groups, so for completeness, we also applied a beta dispersion test (Table 1). The highest R^2 (0.32, Adonis result, Table 1, $p = 0.00$) was between mixed layer and fast-sinking particles (thin red line Figure 4d), emphasizing that these two particle fractions were the most different in terms of particle lipid composition. This result can be explained using the relative contribution of different lipid classes (Figure 3), where unsaturated fatty acids dominated mixed layer particles and sterols dominated fast-sinking particles. Further evidence of differences between these two particle fractions is given by the NMDS plots (Figure 4) that show mixed layer and fast-sinking lipid samples created distinct clusters. The Adonis result may be partly affected by the different distributions of mixed layer and fast-sinking samples (i.e., the size of the mixed layer [red] polygon in Figure 4a is smaller than the fast-sinking [green] polygon). In comparison, the distributions of samples for slow-sinking and suspended particles were also statistically different (beta distribution $p < 0.05$, Table 1, different size polygons in Figure 4a); however, the R^2 for the Adonis test was much lower (0.08) with weaker significance ($p = 0.04$), and in all NMDS plots, the samples overlapped. Hence, we conclude that although the differences in lipid composition between slow-sinking and suspended particles were significant, they were much less

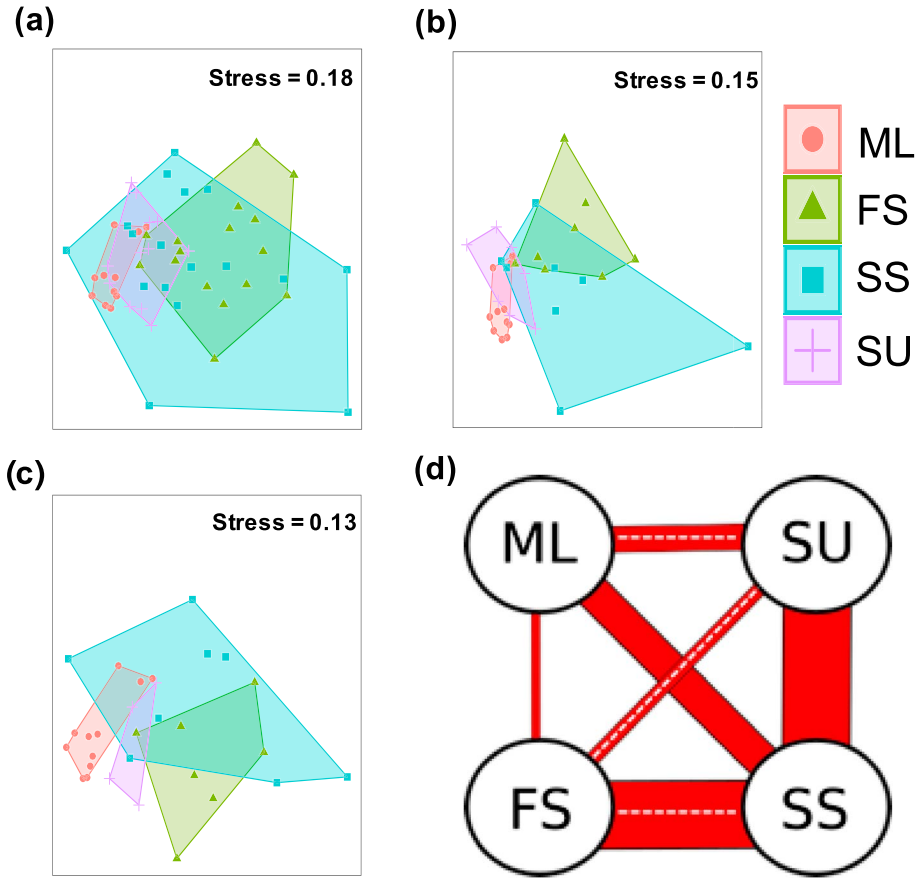

Figure 4. Relationship of lipid compositions between particle fractions. (a–c) Numerical multidimensional scaling (NMDS) plots of lipid compositions between each fraction; ML (mixed layer; red points and polygon), FS (fast-sinking; green triangles and polygon), SS (slow-sinking; blue squares and polygon), and SU (suspended; purple crosses and polygon) particles at (a) all depths, (b) between 40 and 150 m, and (c) between 150 and 350 m. The stress is the measure of scatter about the regression, and a lower stress signifies better representation. (d) Schematic of the results of the Adonis test (Table 1). The wider the red line, the more statistically similar the lipid compositions are. The width represents the R^2 values from the Adonis (analysis of dissimilarities) test, such that a wide red line indicates particle fractions are similar in composition (few dissimilarities, low $R^2 < 0.1$) compared to thin lines where fractions are most different (more dissimilarities, higher $R^2 > 0.25$). All Adonis results were significant to at least $p < 0.05$ or lower. Fast-sinking particles were most similar to slow sinking, then suspended and least similar to mixed layer particles. The Adonis test assumes a homogenous beta distribution (variance) of samples between groups. For completeness, where this condition was met has been indicated by the white-dashed lines (where $p > 0.05$ in the beta distribution test). The NMDS plots show mixed layer and exported fast-sinking particles form distinct clusters according to lipid compositions, which is reiterated by the Adonis result with high dissimilarity between these two particle fractions (thin red connecting line in (d)).

pronounced. Figures 4b and 4c highlight that these patterns are conserved with depth, thus occurring throughout the upper mesopelagic zone.

4. Discussion

We collected organic particles in the mixed layer and mesopelagic zone in the ETNP to determine particle composition. Mixed layer particles were dominated by relatively labile, energy-rich lipids which we propose give evidence to the dominance of cyanobacteria cells in the upper ocean (Volkman et al., 1989). Exported fast-sinking particles below the mixed layer, on the other hand, were dominated by lipids indicative of heterotrophy such as cholesterol (Cavagna et al., 2013) and hence more degraded and refractory than those in the mixed layer. Cholesterol is often instantly associated with herbivorous, crustaceous zooplankton (Grice et al., 1998) as it is not synthesized by most phytoplankton, including cyanobacteria, in which sterols are in very low abundance (Elert et al., 2003). However, it can be associated with any heterotrophic

eukaryote including gelatinous zooplankton such as salps (Phleger et al., 2000) and therefore in the context of this study is assumed not to be solely derived from crustaceous herbivores.

The patterns we observed in particulate lipids versus depth (i.e., lipids becoming more degraded with depth) have been observed frequently in many oceanic settings including oxygen minimum zones (OMZs; Close et al., 2014; Mayzaud et al., 2014; Wakeham & Canuel, 1988; Wakeham & Lee, 1989). However, this is one of the first studies to collect different sinking particulate fractions using the same (MSC) or very similar (MSC and Niskin bottles) methods, at the same depths, over the same time period and without particle fixation or treatment. During the VERTEX cruises in the ETNP in 1981 and 1982 a similar result was found, that suspended particles (collected by in situ pumps) were more labile than larger sinking particles (collected by sediment traps) indicative of undegraded phytoplankton cells compared to the "intensely altered" sinking particles (Wakeham & Canuel, 1988). However, as these were collected using different methods even within the same study, it is difficult to draw accurate conclusions on the state of particle lipids without accounting for some differences due to sampling protocols. Additionally, the sediment trap samples were fixed with mercuric chloride, whereas the in situ pumps were not fixed, possibly leading to further discrepancies between particle fractions. Nevertheless, more recent studies have reiterated the finding that that larger, fast-sinking particles in the ETNP are more refractory than smaller, slow-sinking particles as determined from C:N ratios (Puigcorbé et al., 2015) and microbial POC turnover (Cavan, Trimmer, et al., 2017). The highly refractory composition of the large, fast-sinking particles combined with the reduced crustaceous zooplankton-particle interactions Cavan, Trimmer, et al., 2017) shed light on why POC transfer efficiency is high in low latitudes and particularly through OMZs.

The biochemical composition of sinking particles in this study is also relevant to benthic-pelagic coupling; it could explain why beneath highly productive areas abyssal macrofauna abundance is 1,000× higher than oligotrophic regions (Hardy et al., 2015) but the downward POC flux that feeds these organisms is only up to 7× higher (Henson et al., 2012). Previously, the reduced particle flux was thought to cause this (Thurston et al., 1998); however, our results suggest that the quality (not absolute flux) of the material is reduced where small phytoplankton dominate and that benthic faunal abundance is therefore disproportionately low relative to regions where more labile, energy-rich fast-sinking particles dominate (Billett et al., 1983). It is important to note that while small phytoplankton likely dominated the community composition, this coastal upwelling region is not oligotrophic as surface chlorophyll *a* concentrations reached 1 $\mu g\ L^{-1}$ (Figure 1a) and mixed layer concentrations were even higher at up to 3 $\mu g\ L^{-1}$ (Figure S1).

We can say with high certainty (similar distribution of samples, beta dispersion test $p > 0.05$) that fast-sinking particles were most similar to slow-sinking ($R^2 = 0.07$, thick red line Figure 4d), which were also similar to suspended particles ($R^2 = 0.08$). The latter is not a surprising result as the base of the MSC containing slow-sinking particles also contained (by definition) suspended particles. Suspended particles were similar to mixed layer particles ($R^2 = 0.13$) but less so to fast-sinking particles ($R^2 = 0.23$, Figure 4d). This reiterates the pattern we observed in lipid composition in Figure 3 where unsaturated fatty acids decrease and sterols increase from mixed-layer to fast-sinking particles. Hence, these two particle fractions are the two end-member groups in terms of lipid composition (mixed-layer > suspended > slow-sinking > fast-sinking).

We propose that fast-sinking particles in the upper mesopelagic zone in the ETNP are not rapidly formed from the direct aggregation of phytoplankton in the mixed layer as observed in many other oceanic regions, but through a slower, more inefficient process of the aggregation of small phytoplankton cells into small, suspended, and slow-sinking particles, which, in turn, aggregate to form larger fast-sinking particles. Once a certain density and size threshold is met, the fast-sinking particles sink out of the mixed layer through gravitational settling, whereas slow-sinking particles are likely advected from the mixed layer. This contradicts knowledge gained from temperate and polar regions where small, slow-sinking, and suspended particles are formed solely from the fragmentation of larger, fast-sinking particles (Baker et al., 2017; Mayor et al., 2014). We believe that fragmentation is still an important process in producing labile, slow-sinking particles in the deeper mesopelagic and below, but in the upper mesopelagic and mixed layer, the slow-sinking particles are more important in aggregation processes. The dominance of smaller phytoplankton overlying these waters results in a high export of slow sinking particles (Puigcorbé et al., 2015) and hence is also prominent in the oligotrophic subtropical gyres (Hung et al., 2010) and eutrophic equatorial coastal regions such as the ETNP in this study. The rapid turnover of smaller, slow-sinking particles (Cavan, Trimmer, et al., 2017) means

that this process likely only occurs in lower-latitude regions where seasonality is reduced. Hence we propose that the near-constant rate of primary production (Brown et al., 2014) allows larger particles to from continuously throughout the year, before the microbes respire all the organic carbon in the smaller particles. For this to occur, particle formation must exceed particle remineralization and degradation.

While our data indicate the presence of an alternative particle formation pathway, we are unable to ascertain exactly how this pathway occurs. We can say with some certainty that crustaceous herbivore (e.g., copepod or Euphausiid) zooplankton-mediated aggregation through the repackaging of phytoplankton cells into fast-sinking fecal pellets is likely not the main driver here as (1) crustaceous zooplankton fecal pellets only formed 14% of the fast-sinking particles, whereas phytodetrital particles (e.g., aggregates or cells) formed 69% of this particle fraction; (2) there was a complete lack of characteristic crustacean zooplankton biomarkers ($C_{20:1}$ and $C_{22:1}$ alcohols or fatty acids; Dalsgaard et al., 2003) in the lipids; and (3) parallel measurements of respiration showed that microbial respiration was the dominant process for particle remineralization (Cavan, Trimmer, et al., 2017), as the low oxygen waters are a hostile environment for zooplankton (Hauss et al., 2016).

We hypothesize in this low oxygen region that gelatinous material might be key for the aggregation of smaller particles before they are respired. We identified that gelatinous aggregates were present during our study (Table S1) but did not have the resources available to fully quantify this. Nevertheless, the lipid composition of gelatinous aggregates is dominated by the fatty acids $C_{16:0}$ and $C_{16:1}$ and the sterol cholesterol (Giani et al., 2012), which were the three most abundant lipids observed in our study (Figure 3). Further evidence of the importance of gelatinous carbohydrates in this region is the low contribution of lipids (1%, this study) and proteins (10%; Van Mooy et al., 2002) to total POC in this region. Sticky carbohydrates such as transparent exopolymer particles (TEPs) can be extremely important in the aggregation of particles in the oceans (Engel & Schartau, 1999; Logan et al., 1995; Passow & Alldredge, 1995). TEPs are produced by phytoplankton or bacteria (Wurl et al., 2011) and enhance aggregation. Noncrustaceous zooplankton such as salps and appendicularia produce other types of gelatinous materials (Alldredge, 1976), which can become incorporated into detrital particles enhancing aggregation particularly below the mixed layer, as is likely to be the case for our aggregates (particularly in Figure 2d). While these organisms were not sampled, salps were clearly visible from the ship in the surface waters and were often caught stuck to the side of the MSC after deployment. Crustaceous zooplankton can break up particles into smaller pieces when they feed, promoting remineralization and decreasing transfer efficiency (Mayor et al., 2014). However, gelatinous zooplankton promote aggregation through the production of sticky gelatinous material (Alldredge, 1976) and production of large, fast-sinking fecal pellets enhancing flux (Wilson et al., 2008); they do not fragment particles. All these processes act to increase transfer efficiency through the mesopelagic zone.

Turnover of unsaturated fatty acids (Figures 3b and 3e) by bacteria could also have contributed to the pronounced increase in the relative importance of sterols with depth. Branched fatty acids are lipid biomarkers for bacteria but are always in very low abundance in particulate lipids (Wakeham, 1995) compared to other compounds and therefore are not a useful tool for assessing the contribution of bacteria to compound synthesis. In this study the contribution of branched fatty acids to total lipids was $<0.5\%$ and they were not included in our statistical analysis. Different tools would be needed to determine the relative importance of bacteria in particle aggregation-disaggregation processes; however, their role in nutrient cycling within OMZs (Wright et al., 2012) and as previously discussed, the production of TEP (Wurl et al., 2011), is well known.

In regions where smaller phytoplankton species dominate, most nutrients are recycled through the microbial loop (Azam et al., 1983). We propose that the enhanced microbial (bacterial) loop and the dominance of cyanobacteria and gelatinous zooplankton in the ETNP and OMZs relative to higher latitudes results in this alternative particle formation pathway observed in this study. The magnitude of this alternative pathway of particle formation may increase as tropical regions and OMZs expand with future climate change. The significant contribution of rapidly recycled slow-sinking particles to total flux in these regions (Cavan, Trimmer, et al., 2017) suggests that a high proportion of primary production is remineralized and respired back to carbon dioxide in the upper ocean above the permanent thermocline, even though the transfer efficiency of fast-sinking particles is high. Thus, carbon dioxide could be readily mixed back to the surface and reexchanged with the atmosphere.

5. Conclusions

Sinking organic particles in the oceans are one of the main sinks of carbon globally and are capable of storing atmospheric carbon in the deep ocean and sediments on long time scales. We collected four particle fractions from the ETNP (a full-range distribution of mixed layer particles and exported suspended, slow- and fast-sinking particles) to measure lipid composition to identify how these particles are formed. We expected fast-sinking particles to closely match the composition of particles in the mixed layer, as observed in temperate and polar regions. However, we observed the opposite so that fast-sinking particles were the most dissimilar to those in the mixed layer and are end-member products formed from the aggregation of intermediary suspended and slow-sinking particles. The lack of crustaceous zooplankton-mediated particle processing in this low oxygen region suggests that microbes and gelatinous zooplankton could be the driving force of this alternative particle formation pathway. Our data are the first of its kind to collect suspended and sinking particles using the same method, so we do not know whether this alternative route of particle formation exists elsewhere, or are limited to areas dominated by small phytoplankton species. We may be currently overestimating the ability of the oceans to store carbon in areas where slow-sinking particles dominate particle export and fast-sinking particles are highly degraded within the first few 100 m of the oceans.

Acknowledgments

We wish to thank the Guatemalan government and their Navy for access to their territorial waters. We are grateful to the crew for their support during cruise JC097 onboard the RRS *James Cook*. We also thank Anu Thompson for her help with lipid extractions and GCMS analysis. This work was funded by a NERC standard grant, NE/EO1559X/1. The authors declare no competing financial issues. The particle lipid data to produce Figures 3 and 4 are available in the supporting information. E.L.C., G.W., and R.S. designed the study. E.L.C. and M.T. collected the particles, and E.L.C. did the lipid extractions and analyzed the data with inputs from S.G. E.L.C. and S.G. wrote the manuscript with contributions from all coauthors.

References

Abramson, L., Lee, C., Liu, Z., Wakeham, S., & Szlosek, J. (2010). Exchange between suspended and sinking particles in the northwest Mediterranean as inferred from the organic composition of in situ pump and sediment trap samples. *Limnology and Oceanography*, *55*(2), 725–739. https://doi.org/10.4319/lo.2009.55.2.0725

Alldredge, A. (1976). Discarded appendicularian houses as sources of food, surface habitats, and particulate organic matter in planktonic environments. *Limnology and Oceanography*, *21*(1), 14–24. https://doi.org/10.4319/lo.1976.21.1.0014

Alldredge, A., & Gotschalk, C. (1988). In situ settling behaviour of marine snow. *Limnology and Oceanography*, *33*(3), 339–351. https://doi.org/10.4319/lo.1988.33.3.0339

Alonso-Gonzalez, I. J., Aristegui, J., Lee, C., Sanchez-Vidal, A., Calafat, A., Fabres, J., et al. (2010). Role of slowly settling particles in the ocean carbon cycle. *Geophysical Research Letters*, *37*, L13608. https://doi.org/10.1029/2010GL043827

Anderson, M. J. (2001). A new method for non-parametric multivariate analysis of variance. *Austral Ecology*, *26*(1), 32–46. https://doi.org/10.1111/j.1442-9993.2001.01070.pp.x

Azam, F., Fenche, T., Field, J. G., Gra, J. S., Meyer-Rei, L. A., & Thingstad, F. (1983). The ecological role of water—Column microbes in the sea. *Marine Ecology Progress Series*, *10*(November 2015), 257–263. https://doi.org/10.3354/meps010257

Bach, L. T., Riebesell, U., Sett, S., Febiri, S., Rzepka, P., & Schulz, K. G. (2012). An approach for particle sinking velocity measurements in the 3–400 μm size range and considerations on the effect of temperature on sinking rates. *Marine Biology*, *159*(8), 1853–1864. https://doi.org/10.1007/s00227-012-1945-2

Baker, C. A., Henson, S. A., Cavan, E. L., Giering, S. L. C., Yool, A., Gehlen, M., et al. (2017). Slow-sinking particulate organic carbon in the Atlantic Ocean: Magnitude, flux, and potential controls. *Global Biogeochemical Cycles*, *31*, 1051–1065. https://doi.org/10.1002/2017GB005638

Becquevort, S., & Smith, W. (2001). Aggregation, sedimentation and biodegradability of phytoplankton-derived material during spring in the Ross Sea, Antarctica. *Deep Sea Research Part II: Topical Studies in Oceanography*, *48*(19–20), 4155–4178. https://doi.org/10.1016/S0967-0645(01)00084-4

Belcher, A., Iversen, M., Giering, S., Riou, V., Henson, S., & Sanders, R. (2016). Depth-resolved particle associated microbial respiration in the Northeast Atlantic. *Biogeosciences Discussions*, *13*, 1–31. https://doi.org/10.5194/bg-2016-130

Belcher, A., Iversen, M. H., Manno, C., Henson, S. A., Tarling, G. A., & Sanders, R. (2016). The role of particle associated microbes in remineralisation of faecal pellets in the upper mesopelagic of the Scotia Sea, Antarctica. *Limnology and Oceanography*, *61*(3), 1049–1064. https://doi.org/10.1002/lno.10269

Billett, D., Lampitt, R., & Rice, A. (1983). Seasonal sedimentation of phytoplankton to the deep-sea benthos. *Nature*, *302*(5908), 520–522. https://doi.org/10.1038/302520a0

Brown, C. W., Schollaert Uz, S., & Corliss, B. H. (2014). Seasonality of oceanic primary production and its interannual variability from 1998 to 2007. *Deep Sea Research Part I: Oceanographic Research Papers*, *90*(supplement C), 166–175. https://doi.org/10.1016/j.dsr.2014.05.009

Buesseler, K., Bacon, M., Cochran, J., & Livingston, H. (1992). Carbon and nitrogen export during the JGOFS North Atlantic Bloom Experiment estimated from 234Th:238U disequilibria. *Deep Sea Research, Part I*, *39*(7–8), 1115–1137. https://doi.org/10.1016/0198-0149(92)90060-7

Buesseler, K., Ball, L., Andrews, J., Cochran, J. K., Hirschberg, D. J., Bacon, M. P., et al. (2001). Upper Ocean export of particulate organic carbon and biogenic silica in the Southern Ocean along 170 degrees W. *Deep Sea Research, Part II*, *48*(19–20), 4275–4297. https://doi.org/10.1016/S0967-0645(01)00089-3

Cavagna, A.-J., Dehairs, F., Bouillon, S., Woule-Ebongué, V., Planchon, F., Delille, B., & Bouloubassi, I. (2013). Water column distribution and carbon isotopic signal of cholesterol, brassicasterol and particulate organic carbon in the Atlantic sector of the Southern Ocean. *Biogeosciences*, *10*(4), 2787–2801. https://doi.org/10.5194/bg-10-2787-2013

Cavan, E. L., Henson, S. A., Belcher, A., & Sanders, R. (2017). Role of zooplankton in determining the efficiency of the biological carbon pump. *Biogeosciences*, *14*, 1–25. https://doi.org/10.5194/bg-2016-251

Cavan, E. L., Le Moigne, F. A. C., Poulton, A. J., Tarling, G. A., Ward, P., Daniels, C. J., et al. (2015). Attenuation of particulate organic carbon flux in the Scotia Sea, Southern Ocean, is controlled by zooplankton fecal pellets. *Geophysical Research Letters*, *42*, 821–830. https://doi.org/10.1002/2014GL062744

Cavan, E. L., Trimmer, M., Shelley, F., & Sanders, R. (2017). Remineralization of particulate organic carbon in an ocean oxygen minimum zone. *Nature Communications*, *8*(May 2016), 1–9. https://doi.org/10.1038/ncomms14847

Close, H. G., Wakeham, S. G., & Pearson, A. (2014). Lipid and 13C signatures of submicron and suspended particulate organic matter in the Eastern Tropical North Pacific: Implications for the contribution of Bacteria. *Deep Sea Research Part I: Oceanographic Research Papers*, *85*, 15–34. https://doi.org/10.1016/j.dsr.2013.11.005

Dalsgaard, J., St. John, M., Kattner, G., Muller-Navarra, D., & Hagen, W. (2003). Fatty acid trophic markers in the pelagic marine environment. *Advances in Marine Biology*, *46*, 225–340. https://doi.org/10.1016/S0065-2881(03)46005-7

Durkin, C. A., Estapa, M. L., & Buesseler, K. O. (2015). Observations of carbon export by small sinking particles in the upper mesopelagic. *Marine Chemistry*, *175*, 72–81. https://doi.org/10.1016/j.marchem.2015.02.011

Elert, E. V., Martin-Creuzburg, D., & Le Coz, J. R. (2003). Absence of sterols constrains carbon transfer between cyanobacteria and a freshwater herbivore (< em> Daphnia galeata). *Proceedings of the Royal Society of London. Series B: Biological Sciences*, *270*(1520), 1209 LP–1214. Retrieved from http://rspb.royalsocietypublishing.org/content/270/1520/1209.abstract

Engel, A., & Schartau, M. (1999). Influence of transparent exopolymer particles (TEP) on sinking velocity of Nitzschia closterium aggregates. *Marine Ecology-Progress Series*, *182*, 69–76. https://doi.org/10.3354/meps182069

Eppley, R., & Peterson, B. (1979). Particulate organic matter flux and planktonic new production in the deep ocean. *Nature*, *282*(5740), 677–680. https://doi.org/10.1038/282677a0

Giani, M., Sist, P., Berto, D., Serrazanetti, G. P., Ventrella, V., & Urbani, R. (2012). The organic matrix of pelagic mucilaginous aggregates in the Tyrrhenian Sea (Mediterranean Sea). *Marine Chemistry*, *132–133*, 83–94. https://doi.org/10.1016/j.marchem.2012.01.002

Giering, S., Sanders, R., Lampitt, R., Anderson, T., Tamburini, C., Boutrif, M., et al. (2014). Reconciliation of the carbon budget in the ocean's twilight zone. *Nature*, *507*(7493), 480–483. https://doi.org/10.1038/nature13123

Giering, S., Sanders, R., Martin, A. P., Henson, S. A., Riley, J. S., Marsay, C. M., & Johns, D. G. (2017). Particle flux in the oceans: Challenging the steady state assumption. *Global Biogeochemical Cycles*, *31*, 159–171. https://doi.org/10.1002/2016GB005424

Goericke, R., Olson, R., & Shalapyonok, A. (2000). A novel niche for Prochlorococcus sp. in low-light suboxic environments in the Arabian Sea and the Eastern Tropical North Pacific. *Deep Sea Research Part I: Oceanographic Research Papers*, *47*(7), 1183–1205. https://doi.org/10.1016/S0967-0637(99)00108-9

Graf, G. (1989). Benthic-pelagic coupling in a deep-sea benthic community. *Nature*, *340*(6231), 301–303. https://doi.org/10.1038/340301a0

Grice, K., Klein Breteler, W. C. M., Schouten, S., Grossi, V., deLeeuw, J. W., & Damsté, J. S. S. (1998). Effects of zooplankton herbivory on biomarker proxy records. *Paleoceanography*, *13*(6), 686–693. https://doi.org/10.1029/98PA01871

Hardy, S. M., Smith, C. R., & Thurnherr, A. M. (2015). Can the source–sink hypothesis explain macrofaunal abundance patterns in the abyss? A modelling test. *Proceedings of the Royal Society B: Biological Sciences*, *282*, 20150193. https://doi.org/10.1098/rspb.2015.0193

Hauss, H., Christiansen, S., Schütte, F., Kiko, R., Edvam Lima, M., Rodrigues, E., et al. (2016). Dead zone or oasis in the open ocean? Zooplankton distribution and migration in low-oxygen modewater eddies. *Biogeosciences*, *13*(6), 1977–1989. https://doi.org/10.5194/bg-13-1977-2016

Henson, S., Sanders, R., & Madsen, E. (2012). Global patterns in efficiency of particulate organic carbon export and transfer to the deep ocean. *Global Biogeochemical Cycles*, *26*, GB1028. https://doi.org/10.1029/2011GB004099

Hung, C. C., Xu, C., Santschi, P. H., Zhang, S. J., Schwehr, K. A., Quigg, A., et al. (2010). Comparative evaluation of sediment trap and 234Th-derived POC fluxes from the upper oligotrophic waters of the gulf of Mexico and the subtropical northwestern Pacific Ocean. *Marine Chemistry*, *121*(1-4), 132–144. https://doi.org/10.1016/j.marchem.2010.03.011

Kates, M., & Volcani, B. (1966). Lipid components of diatoms. *Biochimica et Biophysica Acta*, *116*(2), 264–278. https://doi.org/10.1016/0005-2760(66)90009-9

Kiriakoulakis, K., Bett, B. J., White, M., & Wolff, G. A. (2004). Organic biogeochemistry of the Darwin Mounds, a deep-water coral ecosystem, of the NE Atlantic. *Deep Sea Research Part I: Oceanographic Research Papers*, *51*(12), 1937–1954. https://doi.org/10.1016/j.dsr.2004.07.010

Kwon, E., Primeau, F., & Sarmiento, J. (2009). The impact of remineralization depth on the air-sea carbon balance. *Nature Geoscience*, *2*(9), 630–635. https://doi.org/10.1038/ngeo612

Laufkötter, C., Vogt, M., Gruber, N., Aumont, O., Bopp, L., Doney, S. C., et al. (2016). Projected decreases in future marine export production: The role of the carbon flux through the upper ocean ecosystem. *Biogeosciences*, *13*(13), 4023–4047. https://doi.org/10.5194/bg-13-4023-2016

Logan, B. E., Passow, U., Alldredge, A. L., Grossart, H. P., & Simon, M. (1995). Rapid formation and sedimentation of large aggregates is predictable from coagulation rates (half-lives) of transparent exopolymer particles (Tep). *Deep Sea Research Part II: Topical Studies in Oceanography*, *42*(1), 203–214. https://doi.org/10.1016/0967-0645(95)00012-F

Malone, T. C. (1971). The relative importance of nanoplankton and net plankton as primary producers in tropical, oceanic and neritic phytoplankton communities. *Limnology and Oceanography*, *16*(4), 633–639. https://doi.org/10.4319/lo.1971.16.4.0633

Mansour, M. P., Volkman, J. K., Jackson, A., & Blackburn, S. I. (1999). The fatty acid and sterol composition of five marine dinoflagellates. *Journal of Phycology*, *35*(4), 710–720. https://doi.org/10.1046/j.1529-8817.1999.3540710.x

Mayor, D. J., Sanders, R., Giering, S. L. C., & Anderson, T. R. (2014). Microbial gardening in the ocean's twilight zone. *BioEssays: News and Reviews in Molecular, Cellular and Developmental Biology*, *36*(12), 1132–1137. https://doi.org/10.1002/bies.201400100

Mayzaud, P., Boutoute, M., Gasparini, S., & Mousseau, L. (2014). Lipids and fatty acid composition of particulate matter in the North Atlantic: Importance of spatial heterogeneity, season and community structure. *Marine Biology*, *161*(9), 1951–1971. https://doi.org/10.1007/s00227-014-2476-9

Parekh, P., Dutkiewicz, S., Follows, M. J., & Ito, T. (2006). Atmospheric carbon dioxide in a less dusty world. *Geophysical Research Letters*, *33*, L03610. https://doi.org/10.1029/2005GL025098

Passow, U., & Alldredge, A. L. (1995). Aggregation of a diatom bloom in a mesocosm—The role of transparent exopolymer particles (Tep). *Deep Sea Research Part II: Topical Studies in Oceanography*, *42*(1), 99–109. https://doi.org/10.1016/0967-0645(95)00006-C

Phleger, C. F., Nelson, M. M., Mooney, B., & Nichols, P. D. (2000). Lipids of Antarctic salps and their commensal hyperiid amphipods. *Polar Biology*, *23*(5), 329–337. https://doi.org/10.1007/s003000050452

Puigcorbé, V., Benitez-Nelson, C. R., Masqué, P., Verdeny, E., White, A. E., Popp, B. N., et al. (2015). Small phytoplankton drive high summertime carbon and nutrient export in the Gulf of California and Eastern Tropical North Pacific. *Global Biogeochemical Cycles*, *29*, 1309–1332. https://doi.org/10.1002/2015GB005134

R Development Core Team (2017). *R: A language and environment for statistical computing*. Vienna: R Foundation for Statistical Computing. Retrieved from https://www.r-project.org/

Riley, J., Sanders, R., Marsay, C., Le Moigne, F., Achterberg, E., & Poulton, A. (2012). The relative contribution of fast and slow sinking particles to ocean carbon export. *Global Biogeochemical Cycles*, *26*, GB1026. https://doi.org/10.1029/2011GB004085

Sallal, A. K., Nimer, N. A., & Radwan, S. S. (1990). Lipid and fatty acid composition of freshwater cyanobacteria. *Journal of General Microbiology*, *136*(10), 2043–2048. https://doi.org/10.1099/00221287-136-10-2043

Salter, I., Kemp, A. E. S., Moore, C. M., Lampitt, R. S., Wolff, G. a., & Holtvoeth, J. (2012). Diatom resting spore ecology drives enhanced carbon export from a naturally iron-fertilized bloom in the Southern Ocean. *Global Biogeochemical Cycles*, *26*, GB1014. https://doi.org/10.1029/2010GB003977

Sheridan, C. C., Lee, C., Wakeham, S. G., & Bishop, J. K. B. (2002). Suspended particle organic composition and cycling in surface and mid-waters of the equatorial Pacific Ocean. *Deep Sea Research Part I: Oceanographic Research Papers*, *49*(11), 1983–2008. https://doi.org/10.1016/S0967-0637(02)00118-8

Thurston, M. H., Rice, A. L., & Bett, B. J. (1998). Latitudinal variation in invertebrate megafaunal abundance and biomass in the North Atlantic Ocean Abyss. *Deep Sea Research Part II: Topical Studies in Oceanography*, *45*(1–3), 203–224. https://doi.org/10.1016/S0967-0645(97)00077-5

Van Mooy, B. A. S., Keil, R. G., & Devol, A. H. (2002). Impact of suboxia on sinking particulate organic carbon: Enhanced carbon flux and preferential degradation of amino acids via denitrification. *Geochimica et Cosmochimica Acta*, *66*(3), 457–465. https://doi.org/10.1016/S0016-7037(01)00787-6

Volk, T., & Hoffert, M. (1985). Ocean carbon pumps: Analysis of relative strengths and efficiencies in ocean-driven atmospheric CO2 changes. In *The carbon cycle and atmospheric CO2: Natural variations Archean to present* (pp. 99–110). Washington, DC: American Geophysical Union.

Volkman, J. K., Barrett, S. M., Blackburn, S. I., Mansour, M. P., Sikes, E. L., & Gelin, F. (1998). Microalgal biomarkers: A review of recent research developments. *Organic Geochemistry*, *29*(5-7), 1163–1179. https://doi.org/10.1016/S0146-6380(98)00062-X

Volkman, J. K., Jeffrey, S. W., Nichols, P. D., Rogers, G. I., & Garland, C. D. (1989). Fatty acid and lipid composition of 10 species of microalgae used in mariculture. *Journal of Experimental Marine Biology and Ecology*, *128*(3), 219–240. https://doi.org/10.1016/0022-0981(89)90029-4

Wakeham, S. G. (1995). Lipid biomarkers for heterotrophic alteration of suspended particulate organic matter in oxygenated and anoxic water columns of the ocean. *Deep Sea Research Part I: Oceanographic Research Papers*, *42*(10), 1749–1771. https://doi.org/10.1016/0967-0637(95)00074-G

Wakeham, S. G., & Canuel, E. a. (1988). Organic geochemistry of particulate matter in the Eastern Tropical North Pacific Ocean: Implications for particle dynamics. *Journal of Marine Research*, *46*(1), 183–213. https://doi.org/10.1357/002224088785113748

Wakeham, S. G., & Lee, C. (1989). Organic geochemistry of particulate matter in the ocean: The role of particles in oceanic sedimentary cycles. *Organic Geochemistry*, *14*(1), 83–96. https://doi.org/10.1016/0146-6380(89)90022-3

Wakeham, S. G., Schaffner, C., Giger, W., Boon, J. J., & De Leeuw, J. W. (1979). Perylene in sediments from the Namibian Shelf. *Geochimica et Cosmochimica Acta*, *43*(7), 1141–1144. https://doi.org/10.1016/0016-7037(79)90100-5

Wilson, S., Steinberg, D., & Buesseler, K. (2008). Changes in fecal pellet characteristics with depth as indicators of zooplankton repackaging of particles in the mesopelagic zone of the subtropical and subarctic North Pacific Ocean. *Deep Sea Research Part II: Topical Studies in Oceanography*, *55*(14–15), 1636–1647. https://doi.org/10.1016/j.dsr2.2008.04.019

Wright, J. J., Konwar, K. M., & Hallam, S. J. (2012). Microbial ecology of expanding oxygen minimum zones. *Nature Reviews Microbiology*, *10*(6), 381–394. https://doi.org/10.1038/nrmicro2778

Wurl, O., Miller, L., & Vagle, S. (2011). Production and fate of transparent exopolymer particles in the ocean. *Journal of Geophysical Research*, *116*, C00H13. https://doi.org/10.1029/2011JC007342

Zielinski, U., & Gersonde, R. (1997). Diatom distribution in Southern Ocean surface sediments (Atlantic sector): Implications for paleoenvironmental reconstructions. *Palaeogeography, Palaeoclimatology, Palaeoecology*, *129*(3–4), 213–250. https://doi.org/10.1016/S0031-0182(96)00130-7

Zimmerman, A. R., & Canuel, E. A. (2001). Bulk organic matter and lipid biomarker composition of Chesapeake Bay surficial sediments as indicators of environmental processes. *Estuarine, Coastal and Shelf Science*, *53*(3), 319–341. https://doi.org/10.1006/ecss.2001.0815